Supplemental Material

Supplemental Methods, Figures, Figure Legends and Tables

Supplemental Methods

Magnetic resonance imaging (MRI)

Under 1-2% isoflurane anesthesia, pigs were positioned in the MRI scanner (Signa EXCITE 3T system, GE, Waukeshau, WI) and Blood Oxygen Level Dependent (BOLD) images acquired before and after intravenous injection of adenosine (400 mg/kg/min) through the ear vein catheter.

BOLD images (4-5 axial-oblique) were acquired along the cardiac short axis during suspended respiration. Gated Fast Gradient Echo (FGRE) sequence was used with TR/TE/number of echoes/Matrix size/FOV/Slice thickness/Flip angle= 6.8 ms/1.6-4.8 ms/8/128×128/35/0.5 cm/30°.

The BOLD index, R_2*, was estimated in each voxel by fitting the MR signal intensity vs. echo times to a single exponential function and calculating the MR intensity decay rate. A region of interest in the septum, which is least influenced by air-induced artifacts, was traced in each slice on T_2*-weighted images obtained.

MDCT

64-slice MDCT (Somatom Definition-64, Siemens Medical Solution, Forchheim, Germany) was performed 2 days after MRI to evaluate cardiac structure and function, as shown previously.[1] Briefly, two parallel 6-mm-thick mid-left-ventricle (LV) levels were selected for evaluation of microvascular perfusion and function. A bolus injection of nonionic, low osmolar contrast medium (Isovue-370, 0.33 ml/kg over 2 sec) into the right atrium was followed by a 50-s flow study during respiratory suspension. Fifteen minutes later, this was repeated during a 5-min intravenous infusion of adenosine (400 μg/kg/min). Subsequently, the entire LV was

scanned 20 times throughout the cardiac cycle to obtain cardiac systolic and diastolic functions and LV muscle mass.

Images were analyzed with Analyze™ (Biomedical Imaging Resource, Mayo Clinic, Rochester, MN), as reported previously.[1, 2] For LVMM, the end-diastolic LV endocardial and epicardial borders were traced at each tomographic level to sum the products of myocardial volume and specific gravity.[3] LV cavity was also traced at end-diastole and systole to calculate stroke volume, cardiac output, and LV ejection fraction.[3] Cardiac index was calculated by cardiac output normalized for swine body-surface-area.[4] Early (E) and late (A) LV filling rates were calculated from the positive slopes of the curve, describing the change in LV cavity volume during the cardiac cycle.[3] Myocardial perfusion and microvascular permeability index before and during adenosine infusion were calculated from time-attenuation curves obtained from the anterior cardiac wall ROI, as we previously described.[1-3]

Fat measurement

For pericardial fat volume, regions of interests were traced around the heart on the MDCT-derived cross-sections, and expanded proportionally in 3-dimensions within the chest wall, bordered by the descending thoracic aorta and thoracic musculature. The pericardial fat was then measured based on the attenuation range for fat and expressed as ratio to the entire cardiac volume.

Companies and dilutions for antibodies

Santa Cruz (1:200 for all): vascular endothelial growth factor (VEGF) and its receptor Flk-1, P47, P67, superoxide dismutase (SOD) -1, TNF-α, matrix metalloproteinase (MMP)-2, tissue inhibitor of metalloproteinase (TIMP)-1, and transforming growth-factor (TGF)-β1; Abcam: CD134 (1:500), interleukin (IL)-6 (1:1000), sirtuin 1 (SIRT1, 1:5000), peroxisome proliferator-activated receptor gamma coactivator 1- α (PGC-1α, 1:1000), ATP synthase mitochondrial F1

complex assembly factor 1 (ATPAF1, 1:1000), uncoupling protein-2 (UCP2, 1:500), unc-51-like kinase-1 (ULK1, 1:500), microtubule-associated protein-1 light chain (LC)3 (LC3B, 1:500), and phospho-AMP-activated protein kinase (p-AMPK, 1:1000); Cell Signaling Technology: Beclin-1 (1:1000), autophagy-related gene (Atg) 12 (1:1000), mammalian target of rapamycin (mTOR, 1:1000), and phosphorylated signal-transducer and activator of transcription (STAT)-3 (1:1000); Thermo: C-C motif receptor (CCR)-2 (1:1000), CCAAT/enhancer binding protein (C/EBP) and homologous protein (CHOP, 1:100); Millipore: GP91(1:500); Serotec: CD163(1:20); Novocastra: CD8 (1:20); MyBioSource: monocyte chemoattractant protein (MCP)-1 (1:7500); Alpha Diagnostic International: creatine transporter 1 (CT1, 1:400); BD Biosciences: plasminogen-activator inhibitor (PAI)-1 (1:2500).

Micro-CT

The subepicardial and subendocardial spatial density[5], average diameter, and tortuosity of microvessels were classified using Analyze™ as small (diameters 20-200 μm), medium (201-300 μm), or large (301-500 μm) microvessels.[6] Analysis was performed by an experienced imaging analyst who was blinded to the study groups. In order to minimize the influence of potential variability, the operator combined 2-D and 3-D images to determine the threshold for each sample. Furthermore, similar incremental intervals (about 20 slices) were used to sample 30 representative slices for vessels density measurement.

Supplemental Figures

Figure I.

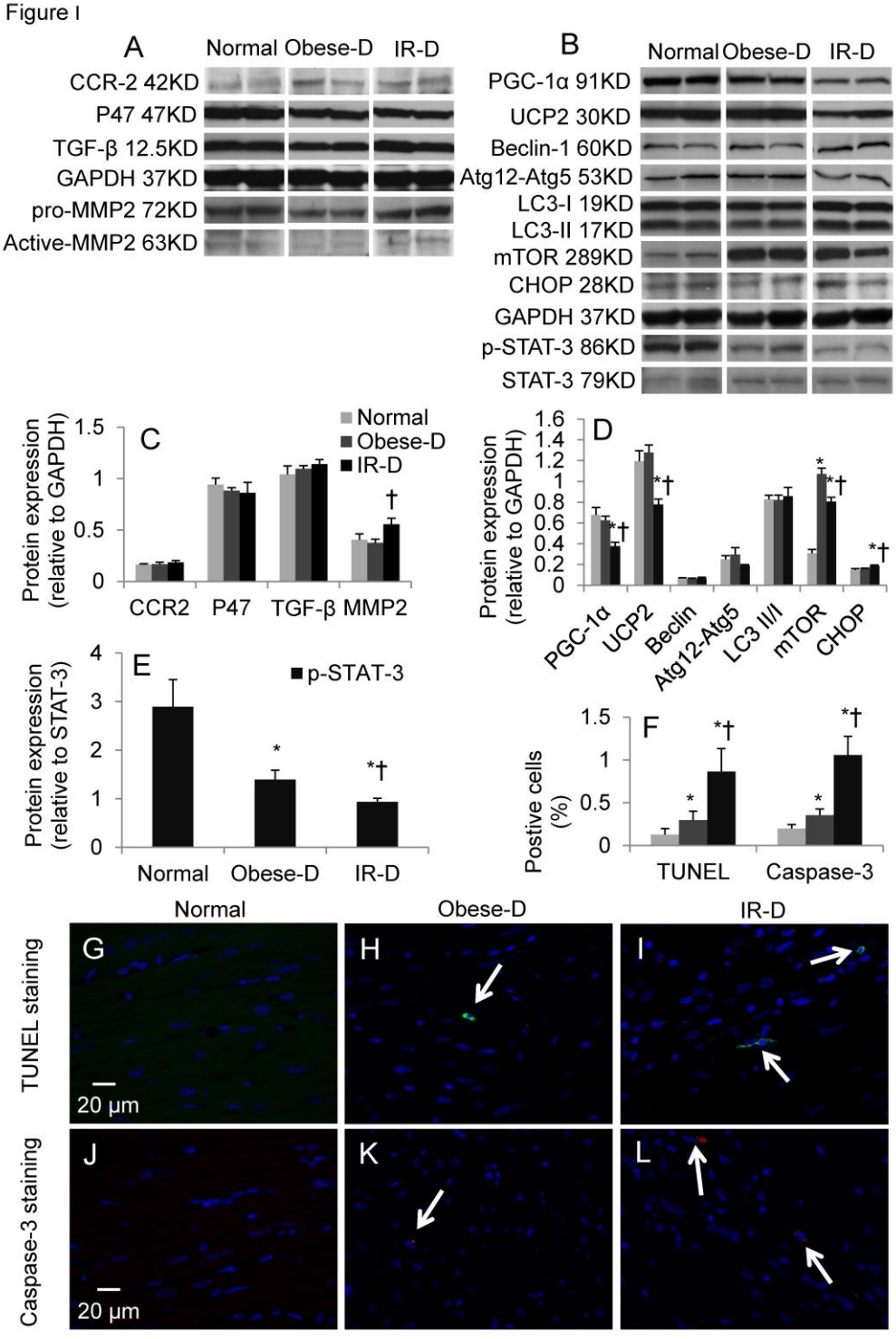

Figure legends

Figure I. Myocardial inflammation, oxidative stress, fibrosis, mitochondrial function, autophagy, and apoptosis in domestic normal, obese, and insulin resistance (IR) pigs. Myocardial protein expression of C-C motif receptor (CCR)-2, P47, transforming growth-factor (TGF)-β1, and matrix metalloproteinase (MMP)-2 (A), and their quantification (C). Myocardial protein expression of peroxisome proliferator-activated receptor gamma coactivator 1-α (PGC-1α), uncoupling protein-2 (UCP2), Beclin-1, conjugated autophagy-related gene (Atg)12-Atg5, microtubule-associated protein-1 light chain 3 (LC3), and mammalian target of rapamycin (mTOR), and apoptosis-related proteins including CCAAT/enhancer binding protein (C/EBP) homologous protein (CHOP) and phosphorylated signal-transducer and activator of transcription (STAT)-3 (B), and their quantifications (D-E). Representative images of TUNEL (G-I), and Caspase-3 (J-L) staining, and their quantifications (F). IR, insulin resistance. (L); $p \leq 0.05$ *vs.* normal, †$p \leq 0.05$ *vs.* obese-D. White arrows indicate positive cells. N=6, 6, and 2 for staining and Western blot. Taken together, these suggested exacerbated inhibition of autophagy and increase in apoptosis in IR-D pigs compared to obese-D pigs.

Supplemental Tables

Table I. Cardiac size (*mean±SEM*) in lean, obese, and MetS Ossabaw pigs.

Cardiac size	Lean (n=6)	Obese (n=6)	MetS (n=6)
LV Volume (ml)			
EDV	37.9±4.3	43.0±3.3	50.2±3.7*
ESV	13.4±1.9	18.3±2.3	17.7±2.9
LA Volume (ml)			
EDV	2.5±0.6	4.0±0.9	2.8±0.3
ESV	7.4±0.7	9.4±0.9	8.7±1.1
LVMM (g)	30.6±2.0	36.4±2.2*	42.2±3.3*
LV wall area (cm^2)			
EDV	44.8±4.9	44.9±2.7	49.3±2.6
ESV	58.2±7.4	58.6±2.2	59.2±3.2

For LV wall area (representing its thickness), comparable LV levels (defined by landmarks) were selected in all pigs during each cardiac phase, yet systole and diastole are not directly compared, as it is difficult to track and ascertain precisely the same level for both cardiac phases. **p≤0.05 vs. lean, †p≤0.05 vs. obese. MetS, metabolic syndrome; LV, left ventricle; EDV, end diastolic volume; ESV, end systolic volume; LVMM, left ventricle muscle mass.*

Table II. Characteristics (*mean±SEM*) of normal, obese-D, and insulin resistance (IR)-D pigs.

	Normal (n=6)	Obese-D (n=6)	IR-D (n=2)
Body weight (kg)	61.9±1.3	69.3±1.5*	68.0±5.0*
Intra-abdominal fat (%)	6.9±0.4	17.1±1.1*	8.2±1.5†
Total cholesterol (mg/dl)	75.8±8.0	126.0±25.1*	598.0±127*†
LDL cholesterol (mg/dl)	35.0±3.0	74.9±75.1	400.4±128.2*†
HDL cholesterol (mg/dl)	39.4±4.6	100.8±22.0*	196.5±1.5*
LDL/HDL	1.2±0.6	1.6±0.3	2.0±0.7
Plasma triglycerides (mg/dl)	24.8±2.1	23.7±5.9	5.5±1.5*
HOMA-IR (µU/ml×mg/dl)	0.8±0.3	1.0±0.3	1.8±0.04*

**p≤0.05 vs. normal, †p≤0.05 vs. obese-D. LDL: low-density lipoprotein; HDL: high-density lipoprotein; HOMA-IR: homeostasis model assessment insulin resistance.*

References

1. Urbieta Caceres VH, Lin J, Zhu XY, Favreau FD, Gibson ME, Crane JA, Lerman A, Lerman LO. Early experimental hypertension preserves the myocardial microvasculature but aggravates cardiac injury distal to chronic coronary artery obstruction. *Am. J. Physiol.-Heart Circul. Physiol.* 2011;300:H693-H701
2. Zhu XY, Daghini E, Chade AR, Versari D, Krier JD, Textor KB, Lerman A, Lerman LO. Myocardial microvascular function during acute coronary artery stenosis: Effect of hypertension and hypercholesterolaemia. *Cardiovasc. Res.* 2009;83:371-380
3. Zhu XY, Daghini E, Chade AR, Napoli C, Ritman EL, Lerman A, Lerman LO. Simvastatin prevents coronary microvascular remodeling in renovascular hypertensive pigs. *J Am Soc Nephrol*. 2007;18:1209-1217
4. Kelley KW, Curtis SE, Marzan GT, Karara HM, Anderson CR. Body surface area of female swine. *J Anim Sci*. 1973;36:927-930
5. Rodriguez-Porcel M, Lerman A, Ritman EL, Wilson SH, Best PJM, Lerman LO. Altered myocardial microvascular 3D architecture in experimental hypercholesterolemia. *Circulation*. 2000;102:2028-2030
6. Zhu XY, Rodriguez-Porcel M, Bentley MD, Chade AR, Sica V, Napoli C, Caplice N, Ritman EL, Lerman A, Lerman LO. Antioxidant intervention attenuates myocardial neovascularization in hypercholesterolemia. *Circulation*. 2004;109:2109-2115